1.21 ± 0.09 (1 σ) and the intercept is -0.21 ± 0.09 (1 σ) (dashed line in Fig. 2). Thus, our model explains about 100% of the ^{36}Cl flux variability, which is in covariance with the magnetic variability. It is rather difficult, however, to interpret the calculated parameter errors in terms of confidence intervals because of the fitted time scale.

The correlation of $r = 0.56$ ($n = 406$) between the unfiltered ^{36}Cl flux and the calculated production rate data indicates that about 30% of the total variance of the unfiltered ^{36}Cl flux can be explained by geomagnetically induced production variations. For low-pass filtered data (frequency = 1/3000 years), the correlation rises to $r = 0.67$. The remaining variance is larger than the experimental errors and therefore still contains information about other paleoenvironmental factors. Changing climatical and meteorological conditions may alter transport, deposition, and concentration of ^{36}Cl in ice. The sedimentation process may affect the record of magnetic intensity; short-time geomagnetic variability cannot be monitored yet by corresponding archives. Cosmic ray intensity as well as solar activity fluctuations have to be taken into account, too.

Thus, our study agrees well with an investigation that attributes the 38-ka ^{10}Be peak in Antarctica to a low value of the geomagnetic field (*3*). This agreement indicates long-range transport of ^{10}Be from lower latitudes to Antarctica during the last glacial. Beryllium-10 studies in Holocene ice reveal a strong local production component in Antarctica (*24*), however. Although not yet conclusive, these results point to a change in the transport pattern of the Southern Hemisphere between the last glacial period and the Holocene.

Our observations support the reliability of marine sediments as recorders of geomagnetic intensity variations; they also provide an independent approach to reconstruct the history of the geomagnetic dipole field.

REFERENCES AND NOTES

1. D. Lal and B. Peters, in *Handbuch der Physik* (Springer-Verlag, Heidelberg, Germany, 1967), vol. 46, pp. 551–612.
2. J. Beer *et al.*, *Nature* **331**, 675 (1988).
3. A. Mazaud, C. Laj, M. Bender, *Geophys. Res. Lett.* **21**, 337 (1994).
4. C. Robinson, G. M. Raisbeck, F. Yiou, B. Lehman, C. Laj, *Earth Planet. Sci. Lett.* **136**, 551 (1995).
5. S. Baumgartner *et al.*, *J. Geophys. Res.* **102**, 26659 (1997).
6. F. Yiou *et al.*, *ibid.*, p. 26783.
7. R. C. Finkel and K. Nishiizumi, *ibid.*, p. 26699.
8. S. J. Johnsen, W. Dansgaard, J. W. C. White, *Tellus Ser. B* **41**, 452 (1989); C. D. Charles, D. Rind, J. Jouzel, R. D. Koster, R. G. Fairbanks, *Science* **263**, 508 (1994).
9. W. Dansgaard *et al.*, *Nature* **364**, 218 (1993).
10. P. Sharma *et al.*, in *5th International Conference on AMS*, Paris, 23 to 27 October 1990, F. Yiou and G. M. Raisbeck, Eds. (North-Holland, Amsterdam, 1990), pp. 410–415.
11. H. W. Bentley, F. M. Phillips, S. N. Davis, in *Handbook of Environmental Isotope Geochemistry,* P. Fritz and J. C. Fontes, Eds. (Elsevier, Amsterdam, 1986), vol. 2, pp. 427–480.
12. P. M. Grootes, M. Stuiver, J. W. C. White, S. Johnsen, J. Jouzel, *Nature* **366**, 552 (1993).
13. C. U. Hammer and D. A. Meese, *ibid.* **363**, 666 (1993); M. Bender *et al.*, *ibid.* **372**, 663 (1994).
14. E. Tric *et al.*, *J. Geophys. Res.* **97**, 9337 (1992).
15. L. Meynadier, J. P. Valet, R. Weeks, N. J. Shackleton, V. L. Hagee, *Earth Planet. Sci. Lett.* **114**, 39 (1992).
16. J. S. Stoner, J. E. T. Channell, C. Hillaire-Marcel, *ibid.* **134**, 237 (1995).
17. D. A. Schneider, *ibid.* **120**, 301 (1993); B. Lehman *et al.*, *Phys. Earth Planet. Inter.* **93**, 269 (1996); D. V. Kent and N. D. Opdyke, *Nature* **266**, 156 (1977); T. Yamazakia, N. Ioka, N. Eguchi, *Earth Planet. Sci. Lett.* **136**, 525 (1995).
18. Y. Guyodo and J.-P. Valet, *ibid.* **143**, 23 (1996).
19. J. Masarik and J. Beer, in *Proceedings of the 25th International Cosmic Ray Conference*, Space Research Unit, Potchefstroom University, Durban, South Africa, 30 July to 6 August 1997 (Potchefstroom University, Durban, South Africa, 1997), vol. 2, pp. 461–464. In our code, the incident primary cosmic ray particles are transported through the matter considering ionization energy losses and nuclear elastic and inelastic scattering. This code uses only basic physical quantities and parameters, without any free parameters, to numerically simulate all processes relevant in particle production and transport. It enables us to trace the fate of each individual particle and in doing so to study in detail the effects of various parameters on production rates, including geomagnetic field variations. For long-term average solar activity, the dependence of the ^{36}Cl production rate P on the geomagnetic field intensity B can be approximated by the polynomial: $P = 2.11 - 2.81B + 3.17B^2 - 2.09B^3 + 0.73B^4 - 0.10B^5$ (P and B are relative to their present value). The polynomial coefficients are dependent on solar activity and differ slightly for particular isotopes. For weak geomagnetic fields, our model gives production rates that are 15% higher than those from the widely used model of Lal and Peters (*1*).
20. G. M. Raisbeck *et al.*, *Nature* **326**, 273 (1987).
21. J. Beer *et al.*, in *The Last Deglaciation: Absolute and Radiocarbon Chronologies,* E. Bard and W. S. Broecker, Eds. (Springer-Verlag, Berlin, 1992), vol. 12, pp. 141–153.
22. G. C. Castagnoli *et al.*, *Geophys. Res. Lett.* **22**, 707 (1995); L. R. McHargue, P. E. Damon, D. J. Donahue, *ibid.*, p. 659.
23. C. P. Sonett, *Radiocarbon* **34**, 239 (1992).
24. E. Bard, G. M. Raisbeck, F. Yiou, J. Jouzel, *Earth Planet. Sci. Lett.* **150**, 453 (1997); E. J. Steig, P. J. Polissar, M. Stuiver, P. M. Grootes, R. C. Finkel, *Geophys. Res. Lett.* **23**, 523 (1996).
25. We thank the technical staff of the Swiss Federal Institute of Science and Technology, the accelerator group at the Paul Scherrer Institut–Eidgenössische Technische Hochschule accelerator mass spectrometry facility, and the GRIP field team for their help and S. Johnsen for transmitting the δ^{18}O data from the Summit GRIP ice core. Supported by the Swiss National Science Foundation.

16 October 1997; accepted 21 January 1998

Carbonic Acid in the Gas Phase and Its Astrophysical Relevance

Wolfgang Hage, Klaus R. Liedl,* Andreas Hallbrucker, Erwin Mayer*

In outer space, high-energy irradiation of cryogenic ice mixtures of abundant water and carbon dioxide is expected to form solid carbonic acid. Experiments and thermodynamic analyses show that crystalline carbonic acid sublimates without decomposition. Free-energy considerations based on highly accurate molecular quantum mechanics, in combination with vapor pressures resulting from experimental sublimation rates, suggest that in the gas phase, a monomer and dimer of carbonic acid are in equilibrium, comparable to that of formic acid. Gaseous carbonic acid could be present in comets, on Mars and outer solar system bodies, in interstellar icy grains, and in Earth's upper atmosphere.

Carbonic acid (H_2CO_3), the short-lived intermediate in CO_2-HCO_3^-/CO_3^{2-} proton transfer reactions, is a key compound in biological and geochemical carbonate-containing systems (*1–5*). At ambient temperature, H_2CO_3 dissolved in water dissociates rapidly into CO_2 and H_2O, with a rate constant of ~20 s^{-1} and an activation enthalpy of ~70 kJ mol^{-1}; the reaction is highly exergonic (*1–5*). Carbonic acid has recently been synthesized at low temperatures by two basically different routes: (i) high-energy irradiation of cryogenic CO_2/H_2O ice mixtures (*6–9*) and proton-irradiation of pure solid CO_2 (*9*), and (ii) protonation of bicarbonate or carbonate in a new cryogenic technique (*10–14*). Fourier-transform infrared spectroscopic studies led to characterization of two polymorphs. One (β-H_2CO_3) is formed by high-energy irradiation (*6–9*) or by protonation in freeze-concentrated aqueous solution (*11, 13, 14*). The other (α-H_2CO_3) is formed by protonation in methanolic solution (*10–12, 14*), with β-H_2CO_3 transforming into α-H_2CO_3 (*11*). For the gas phase of H_2CO_3, high-level molecular quantum mechanical calcu-

---

Institut für Allgemeine, Anorganische und Theoretische Chemie, Universität Innsbruck, A-6020 Innsbruck, Austria.

*To whom correspondence should be addressed. E-mail: klaus.liedl@uibk.ac.at and erwin.mayer@uibk.ac.at

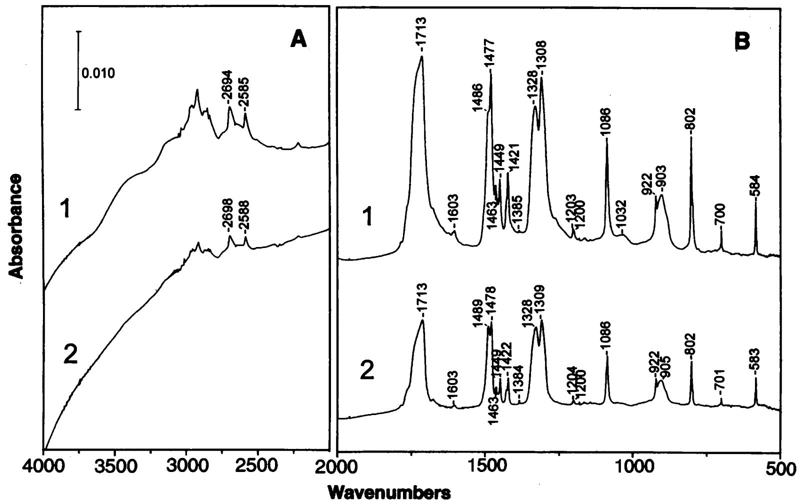

Fig. 1. Sublimation and recondensation of α-H_2CO_3 as seen in infrared spectra (**A**) made by reaction of methanolic solutions of $KHCO_3$ and HCl and recorded in vacuo at 200 K, and (**B**) after sublimation of the H_2CO_3 film and recondensation onto a second window, recorded at 180 K (41). The spectra are shown on the same scale; the ordinate bar is for both 1 and 2 in (A) and (B).

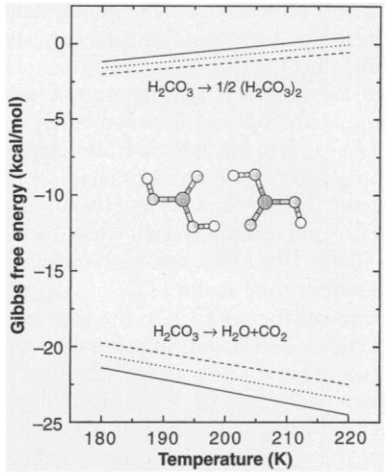

Fig. 2. Gibbs free energy versus temperature of dissociation of H_2CO_3 into CO_2 and H_2O (lower curves) and of dimer formation (upper curves). The partial pressures shown are 10^{-7} mbar (—), 10^{-6} mbar (····), and 10^{-5} mbar (----) for each gas-phase species. The energetics of these species was evaluated by means of a molecular quantum mechanics calculation up to a level of CCSD(T)//6-311++G(3df, 3pd). Frequencies for the calculation of free energies in the gas phase were obtained at MP2/aug-cc-pVDZ level (15).

lations show that hydrogen bonding stabilizes the dimer (15).

We report that α-H_2CO_3 can be sublimated and recondensed without decomposition into CO_2 and H_2O and discuss the significance and implications of solid and gaseous H_2CO_3 for comets, Mars, outer solar system bodies, interstellar icy grains, and our upper atmosphere. To examine the stability of H_2CO_3, we prepared a film of crystalline H_2CO_3 on a CsI window by sequentially depositing layers of glassy methanolic solutions of 0.1 M $KHCO_3$ and of ~2 M HCl in the form of droplets, then by heating in vacuo from 78 to 200 K to induce protonation of HCO_3^- and removal of solvent and excess HCl. The infrared spectrum of the film recorded at 200 K is characteristic for α-H_2CO_3 (Fig. 1, curves 1) (10–12). The high crystallinity of the film is indicated by sharpening of bands and pronounced bandsplitting (12). The HCO_3^- was completely protonated, as indicated by the absence of the intense HCO_3^- band centered at ~1647 cm^{-1} (10, 12). The CsI window with the H_2CO_3 film was removed from the apparatus together with its holder by breaking the vacuum with Ar (99.999%), and it was then stored in liquid N_2.

For the sublimation and recondensation experiment, we placed a second CsI window (window 2) in the infrared beam behind the standard CsI window (window 1) used for protonation of HCO_3^-/CO_3^{2-} and isolation of H_2CO_3. Window 2 was mounted in a copper holder onto the cold finger of a cryostat, which could be regulated from 10 to 320 K (distance to window 1 of ~10 mm). Window 1 with the H_2CO_3 film was then inserted in the apparatus. Traces of ice from the transfer were removed in vacuo from both windows at 200 K. Window 2 was then cooled to ~50 K. On heating window 1 to 220 K, H_2CO_3 sublimated onto window 2 within a few minutes. Thereafter, window 1 was removed from the apparatus. This ensured that the spectrum recorded after removal of window 1 must be from H_2CO_3 that had recondensed on window 2, after sublimation from window 1 (Fig. 1, curves 2).

The spectral features of the film recorded after recondensation are also those of α-H_2CO_3 (Fig. 1, curves 2). Band areas of the spectrum recorded after recondensation are about 50% of those before sublimation (Fig. 1, curves 2 versus curves 1). A broad feature at ~1250 cm^{-1} is caused by a small amount of amorphous or disordered H_2CO_3 (Fig. 1, curve 1B) (12). This feature is absent in the spectrum of the recondensed film (Fig. 1, curve 2B), which indicates a fully crystalline film (10, 12).

Kinetic stability of H_2CO_3 in the gas phase is consistent with theoretical calculations that show that the activation energy for dissociation into CO_2 and H_2O is much higher in the gas phase than it is in aqueous solution. Activation barriers for dehydration of isolated H_2CO_3 of 221 ± 55 kJ mol^{-1} (2) are consistent with recent high-level calculations with a barrier of 174 or 169 kJ mol^{-1} (4, 5). Carbonic acid had been detected in the gas-phase decomposition products of $(NH_4)HCO_3(s)$ by observation of a peak at a mass-to-charge ratio (m/z) = 62 (attributed to $H_2CO_3^+$), with an intensity <1% of the CO_2^+ peak at m/z = 44 (16). But only mass-spectral studies with a pure H_2CO_3 sample could clarify whether the low relative intensity of the $H_2CO_3^+$ peak is caused by fragmentation.

At 200 K, the sublimation rate of α-H_2CO_3 was determined as 1.10^{-8} g cm^{-2} s^{-1} (17). If we assume that this is the theoretical maximum for the sublimation rate (that is, the coefficient of evaporation = 1), then we can estimate by using the Knudsen formula (18) that the saturation vapor pressure, p_s, is 4.10^{-7} mbar for the H_2CO_3 monomer in the gas phase and 3.10^{-7} mbar for the dimer. For ice, a similar p_s value and sublimation rate is obtained at ~160 K (18). This value is consistent with our findings that ice can be removed in vacuo to a large extent before sublimation of α-H_2CO_3 begins (10, 12, 14).

We evaluated the energetics of these species by means of a high-level molecular quantum mechanics calculation. The global minima structures of the monomer and dimer were used in the calculations (the dimer is depicted in Fig. 2). The gas-phase free energy of H_2O, CO_2, H_2CO_3, and its dimer were calculated for the temperature and pressure range relevant for the sublimation experiment, that is, from 180 to 220 K and from 10^{-7} to 10^{-5} mbar pressure for each species. The Gibbs free energy for dissociation of H_2CO_3 into CO_2 and H_2O (Fig. 2, lower curves) obviously disfavors formation of H_2CO_3. This ensures that H_2CO_3 would not recombine if it had decomposed in the gas phase, and it emphasizes the importance of kinetic stabilization. The dimer of H_2CO_3 seems to be slightly favored over the monomer (Fig. 2, upper curves), which is suggestive of the presence of a monomer-dimer mixture in the gas phase, comparable to that in formic acid (*19*).

The astrophysical significance of solid carbonic acid has been discussed before (*3, 8, 9, 11, 13, 20*), but here, we also emphasize the relevance of carbonic acid in the gas phase. Conversion of β-H_2CO_3 into α-H_2CO_3 on astrophysical time scales seems likely, because it can be transformed on laboratory time scales (*11*).

The prevalence of CO_2 in the gases near comet Halley had shown that the cometary nucleus contains CO_2 ice in addition to dominant water ice (*21*). To account for anomalous gas retention and release in comets, the formation of clathrate hydrates in cometary ice, with CO_2 (or other small molecules) as guest, had been suggested (*22*). However, CO_2 clathrate hydrate (CO_2-CH) decomposes into solid CO_2 and H_2O at temperatures below 120 K (*23*). Thus, we propose that formation of solid H_2CO_3 on high-energy irradiation of CO_2-H_2O ices should be considered as an alternative species in comets. Depending on the temperature, solid H_2CO_3 is expected to form first an amorphous solid that crystallizes on heating (*13*). As a comet approaches the sun, the monomer or the dimer of H_2CO_3 will begin to evaporate. These species could be detected once the mass-spectral and spectroscopic patterns of the neutral or ionized species have been determined in the laboratory. Estimates of irradiation doses and penetration depths for comet Halley imply that a layer of solid H_2CO_3 could form on the nuclei's surface (*24*); the thickness of the layer will depend on the type of radiation (*24–26*). This layer would alter and reduce, at a given temperature, gas release of more volatile species underneath that layer [see figure 6 in (*13*)].

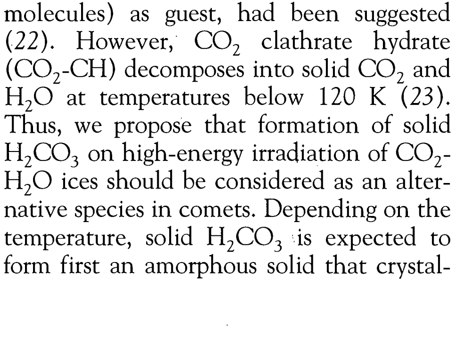

Fig. 3. Comparison of the 2.4- to 5.0-µm wavelength infrared spectral region of comet Halley [curve 1, from (*27*) with its assignment] with that of β-H_2CO_3 recorded at 260 K (curve 2), and those of amorphous and β-H_2CO_3 recorded at 200 and 230 K, respectively (curves 3 and 4). Broken vertical lines indicate possible coincidences. β-H_2CO_3 for curve 2 was made by reaction of aqueous solutions of $KHCO_3$ and HBr [from figure 2, curve 4, in (*13*)], and H_2CO_3 for curves 3 and 4 was made by reaction of aqueous solutions of $KHCO_3$ and HCl [from figure 9 in (*13*)].

In the infrared spectrum of comet Halley and other comets, the characteristic feature at a wavelength of 3.2 to 3.5 µm has been attributed mainly to C-H stretching vibrations of various photoprocessed organic species (*27*). We propose that, in addition, O-H stretching bands of carbonic acid can contribute to this spectral feature (Fig. 3). The spectra of β-H_2CO_3 (Fig. 3, curves 2 and 4) and amorphous H_2CO_3 (curve 3) films show differences in peak shape and intensities beyond those expected for a temperature effect. We attribute these differences to varying amounts of disordered H_2CO_3 or of residual water enclosed in the H_2CO_3 matrix [see figure 6 in (*13*)], or both. Similarly, spectra of H_2CO_3 made by high-energy irradiation of CO_2/H_2O ices or by proton irradiation of solid CO_2 show differences in particular in the O-H stretching band region (*9*). Despite these variations, several of the characteristic features of amorphous and of β-H_2CO_3 agree well with maxima of the comet's spectrum (curve 1, indicated by broken lines). From wavelengths of 6 to 11 µm of the comet's spectrum, the black-body continuum radiation has a maximum and signal-to-noise ratio is low (*26, 27*). Only a weak emission had been marginally observable at 6.8-µm wavelength and was attributed to the vibration frequency of a C-H bond (*27*). Because of these difficulties, the spectral features of amorphous or crystalline H_2CO_3 are unlikely to be observable in this spectral region. Assignment of the 6.8-µm feature to solid H_2CO_3 is also possible because both amorphous H_2CO_3 and the two crystalline forms have an intense band in this spectral region (*10–14*).

On Mars, CO_2 ice, in intimate mixture with or segregated from lower amounts of water ice, is the dominant constituent of the polar caps and of ice particles in the atmosphere (*28, 29*). Formation of CO_2-CH on Mars has been postulated (*22*), but formation of solid H_2CO_3 by high-energy irradiation is an alternative. Because H_2CO_3 can sublimate without decomposition, it can accrete despite cycles of sublimation and condensation on the martian surface (*13, 20*). The combination of low irradiation doses on the martian surface (*20, 30*) and decomposition into CO_2 and H_2O by thermal cycling could otherwise prevent accretion of appreciable quantities of solid H_2CO_3. The infrared spectrum of the Martian surface is similar enough to that of H_2CO_3 that it could occur on the surface or in the atmosphere (*20*).

On many of the outer solar system bodies, water ice is the dominant surface constituent (*29*). Because most of these objects have little or no atmosphere, their surfaces experience high-energy irradiation; therefore, photolysis due to solar ultraviolet radiation and radiolysis occur at the surface (*25*). Thus, solid H_2CO_3 can form on the surface of these icy solar system bodies once sufficient CO_2 ice is present (*29*). Infrared absorption features at 3.4- and 3.88-µm wavelengths observed in the surface materials of the Galilean satellites of Jupiter (*31*) are at similar wavelengths as those of amorphous and β-H_2CO_3 (Fig. 3, curves 2 through 4).

Interstellar icy grains in dense molecular clouds are slowly photoprocessed at <50 K (*28, 32, 33*), and H_2O and CO_2 ices are the major volatile species of the icy-grain mantle (*34–36*). These are optimal conditions for formation of amorphous H_2CO_3 by high-energy irradiation. Formation of solid H_2CO_3 might explain recent infrared spectroscopic studies of puzzling gas:solid ratios in interstellar clouds (*35, 36*). This ratio is much larger for H_2O than for CO_2, although p_s and the rate of sublimation of CO_2 are higher than that of H_2O at a given temperature. However, H_2CO_3 and CO_2 enclosed in a H_2CO_3 matrix sublimate at a higher temperature than water ice [see figures 8 and 9 in (*13*)]. Carbonic acid has been suggested recently as a possible species of interstellar ices (*34*).

Carbonic acid might also form in Earth's atmosphere, most likely in cirrus clouds in the upper troposphere, because temperatures are low, deeply supercooled droplets exist, and H_2O ice and CO_2 are abundant (*29, 37*). Formation from CO_2-H_2O ices is unlikely because of the lack of radiation of sufficient energy (*29*); instead, solid H_2CO_3 might form by protonation of HCO_3^--CO_3^{2-} anions by, for example, HCl. These anions form in atmospheric water droplets from carbonate containing dust or on interaction of NH_3 with CO_2 (*38, 39*). On formation of ice, protonation to solid H_2CO_3 can occur in phase-segregated, freeze-concentrated solution, in a similar manner to the process for formation of β-H_2CO_3 (*11, 13, 14*). Solid H_2CO_3 thus formed is expected to precipitate together with the ice crystals and to decompose on warming into CO_2 and H_2O. However, it is also conceivable that either some gaseous H_2CO_3 or solid H_2CO_3 on fine particles escapes into the stratosphere. Carbon dioxide is chemically inert in the troposphere and stratosphere (*40*). This might be different for (gaseous or solid) H_2CO_3 because its formation from CO_2 and H_2O is highly endergonic (*1–5*, *15*).

Further studies of gaseous H_2CO_3 should concentrate on its mass-spectral and spectroscopic characterization, and on the effects of temperature, vapor pressure, and water vapor on its kinetic stability. These data are essential to the search for gaseous and solid H_2CO_3 in future space missions.

REFERENCES AND NOTES

1. Literature up to 1973 is reviewed in *Gmelin Handbuch der Anorganischen Chemie, Kohlenstoff*, E. H. E. Pietsch and A. Kotowski, Eds. (Teil C3, Verlag Chemie, Weinheim, Germany, 1973), vol. 14, pp. 117–154; D. M. Kern, *J. Chem. Educ.* **37**, 14 (1960); M. Eigen, K. Kustin, G. Maass, *Z. Phys. Chem.* **30**, 130 (1961); Y. Pocker and D. W. Bjorkquist, *J. Am. Chem. Soc.* **99**, 6537 (1977); M. T. Nguyen and T.-K. Ha, *ibid.* **106**, 599 (1984).
2. B. Jönsson *et al.*, *J. Am. Chem. Soc.* **99**, 4628 (1977).
3. R. K. Khanna, J. A. Tossell, K. Fox, *Icarus* **112**, 541 (1994).
4. C. A. Wight and A. I. Boldyrev, *J. Phys. Chem.* **99**, 12125 (1995).
5. M. T. Nguyen, G. Raspoet, L. G. Vanquickenborne, P. Th. Van Duijnen, *J. Phys. Chem. A* **101**, 7379 (1997).
6. M. H. Moore and R. K. Khanna, *Spectrochim. Acta* **47 A**, 255 (1991).
7. ______, B. Donn, *J. Geophys. Res.* **96**, 17541 (1991).
8. N. DelloRusso, R. K. Khanna, M. H. Moore, *ibid.* **98**, 5505 (1993).
9. J. R. Brucato, M. E. Palumbo, G. Strazzulla, *Icarus* **125**, 135 (1997).
10. W. Hage, A. Hallbrucker, E. Mayer, *J. Am. Chem. Soc.* **115**, 8427 (1993).
11. ______, *J. Chem. Soc. Faraday Trans.* **91**, 2823 (1995).
12. ______, *ibid.* **92**, 3183 (1996).
13. ______, *ibid.*, p. 3197.
14. ______, *J. Mol. Struct.* **408/409**, 527 (1997).
15. K. R. Liedl, S. Sekušak, E. Mayer, *J. Am. Chem. Soc.* **119**, 3782 (1997).
16. J. K. Terlouw, C. B. Lebrilla, H. Schwarz, *Angew. Chem. Intl. Ed. Engl.* **26**, 354 (1987); J. K. Terlouw, D. Sülzle, H. Schwarz, *Angew. Chem.* **102**, 431 (1990).
17. The rate of sublimation at 200 K was determined by measuring the percent decrease of band areas of several selected bands of α-H_2CO_3 centered at 1713, 1328/1308, 1086, and 802 cm^{-1}. For a given time, percent decrease of the four bands was the same within ±1% of relative band areas. The amount of sublimated H_2CO_3 was determined in an indirect way by comparing band areas of the composite D_2CO_3 band centered at ~1712 cm^{-1} (ν C = O) with that of the educt band in $KDCO_3$ centered at 1632 cm^{-1} (ν C = O) (*10*). For this comparison, spectra depicted in figure 1b of (*10*) as curves 1 and 5 for reaction in deuterated solution were selected, first, because in deuterated solution, the $KDCO_3$ band at 1632 cm^{-1} does not contain contributions from other bands (for example, the O-H deformation mode), and second, because the 1:1 correspondence between D_2CO_3 and DCO_3^- was established by quantitative conversion and the absence of enclosed CO_2. Band-area ratio was 0.33 for ν C = O (in D_2CO_3)/ν C = O (in DCO_3^-). In a next step, absorbance of the $KHCO_3$ band was determined in a calibrated liquid cell (15.0-μm path length) for 0.10 M $KHCO_3$ dissolved in methanol. This enabled us to determine via the band-area ratio the amount of sublimated H_2CO_3. At 200 K, the rate of H_2CO_3 sublimation was 1.10^{-8} cm^{-2} s^{-1} in this experiment.
18. W. Umrath, *Mikroskopie* **40**, 9 (1983).
19. R. C. Millikan and K. S. Pitzer, *J. Am. Chem. Soc.* **80**, 3515 (1958); T. Miyazawa and K. S. Pitzer, *J. Chem. Phys.* **30**, 1076 (1959); J. E. Bertie and K. H. Michaelian, *ibid.* **76**, 886 (1982); K. I. Lazaar and S. H. Bauer, *J. Am. Chem. Soc.* **107**, 3769 (1985); Y.-T. Chang, Y. Yamaguchi, W. H. Miller, H. F. Schaefer III, *ibid.* **109**, 7245 (1987); G. Henderson, *J. Chem. Educ.* **64**, 88 (1987); I. Yokoyama, Y. Miwa, K. Machida, *J. Am. Chem. Soc.* **113**, 6458 (1991).
20. G. Strazzulla, J. R. Brucato, G. Cimino, M. E. Palumbo, *Planet. Space Sci.* **44**, 1447 (1996).
21. D. Krankowsky *et al.*, *Nature* **321**, 326 (1986); J. Maddox, *ibid.*, p. 366; J. Crovisier *et al.*, *Astron. Astrophys.* **315**, L385 (1996).
22. A. H. Delsemme and P. Swings, *Ann. Astrophys.* **15**, 1 (1952); A. H. Delsemme and D. C. Miller, *Planet. Space Sci.* **18**, 709 (1970); *ibid.*, p. 717; S. L. Miller, in *Physics and Chemistry of Ice*, E. Whalley *et al.*, Eds. (Royal Society of Canada, Ottawa, 1973), pp. 42–50; J. I. Lunine and D. J. Stevenson, *Astrophys. J. Suppl. Ser.* **58**, 493 (1985); S. Engle, J. I. Lunine, J. S. Lewis, *Icarus* **85**, 380 (1990); A. Hallbrucker and E. Mayer, *ibid.* **90**, 176 (1991); D. Blake, L. Allamandola, S. Sandford, D. Hudgins, F. Freund, *Science* **254**, 548 (1991).
23. D. W. Davidson *et al.*, *J. Incl. Phenom.* **2**, 231 (1984).
24. Ch. Chyba and C. Sagan, *Nature* **330**, 350 (1987).
25. R. E. Johnson and T. I. Quickenden, *J. Geophys. Res.* **102**, 10985 (1997); K. Roessler, in *Handbook of Hot Atom Chemistry*, J. P. Adloff, Ed. (Kodansha, Tokyo, 1992), pp. 601–624.
26. M. Combes *et al.*, *Nature* **321**, 266 (1986).
27. M. Combes *et al.*, *Icarus* **76**, 404 (1988).
28. W. Calvin and T. Z. Martin, *J. Geophys. Res.* **99**, 21143 (1994).
29. R. P. Wayne, *Chemistry of the Atmospheres* (Clarendon Press, Oxford, 1995), chaps. 8 and 9.
30. L. C. Simonsen and J. E. Nealy, *NASA Tech. Paper* 3300 (1993).
31. T. B. McCord *et al.*, *Science* **278**, 271 (1997).
32. J. M. Greenberg and L. B. D'Hendecourt, in *Ices in the Solar System*, J. Klinger, D. Benest, A. Dollfus, R. Smoluchowski, Eds. (NATO ASI Series C 156, Reidel, Boston, MA, 1985), pp. 185–204; J. M. Greenberg, C. E. P. M. van de Bult, L. J. Allamandola, *J. Phys. Chem.* **87**, 4243 (1983).
33. For review see: E. Herbst, *Annu. Rev. Phys. Chem.* **46**, 27 (1995).
34. D. C. B. Whittet *et al.*, *Astron. Astrophys.* **315**, L357 (1996).
35. E. F. van Dishoeck *et al.*, *ibid.*, p. L349.
36. Th. de Graauw *et al.*, *ibid.*, p. L345.
37. K. Sassen, K. N. Liou, S. Kinne, M. Griffin, *Science* **227**, 411 (1985); K. Sassen, *ibid.* **257**, 516 (1992).
38. W. Stumm and J. J. Morgan, *Aquatic Chemistry* (Wiley-Interscience, New York, 1996), pp. 206–249.
39. G. P. Ayers, R. W. Gillett, E. R. Caeser, *Tellus B* **37**, 35 (1985).
40. M. J. Molina, L. T. Molina, Ch. E. Kolb, *Annu. Rev. Phys. Chem.* **47**, 327 (1996).
41. Infrared spectra were recorded in transmission on Biorad's FTS 45 at 2 cm^{-1} resolution (DTGS detector, UDR1) by coadding 50 scans. The spectrum of water vapor was subtracted from the spectra.
42. We are grateful to S. Sekušak for help in the early stages of the calculations and to the Forschungsförderungsfonds of Austria for financial support (project P12319-PHY).

26 September 1997; accepted 21 January 1998

Abrupt Climate Events 500,000 to 340,000 Years Ago: Evidence from Subpolar North Atlantic Sediments

D. W. Oppo, J. F. McManus, J. L. Cullen

Subpolar North Atlantic proxy records document millennial-scale climate variations 500,000 to 340,000 years ago. The cycles have an approximately constant pacing that is similar to that documented for the last glacial cycle. These findings suggest that such climate variations are inherent to the late Pleistocene, regardless of glacial state. Sea surface temperature during the warm peak of Marine Isotope Stage 11 (MIS 11) varied by 0.5° to 1°C, less than the 4° to 4.5°C estimated during times of ice growth and the 3°C estimated for glacial maxima. Coherent deep ocean circulation changes were associated with glacial oscillations in sea surface temperature.

During the last glaciation (MIS 2 to 4) and deglaciation, sea surface temperatures (SSTs) oscillated in the subpolar North Atlantic at several time scales. Discrete ice-rafting events marked times of cool SSTs. A series of gradual cooling intervals 6000 to 10,000 years (6 to 10 ky) long were terminated by massive iceberg discharge into the North Atlantic (Heinrich events) (*1–3*). Shorter SST cycles of 2 to 3 ky [Dansgaard-Oeschger cycles (*4*)], each terminated by a cold ice-rafting event, occurred between Heinrich events (*5*). New evidence indicates that there may have been more frequent sea surface changes, spaced ~1.5 ky apart (*6*). A similar hierarchy is emerging from Greenland ice core records: glaciochemical time series indicate that the strength of the polar atmospheric circulation varied over cycles of between 6 and 1.45 ky (*7*), comparable to the approximate spacing of events deduced from the marine record. Such millennial climate oscillations also occurred during the Holocene (*6–8*).

Deep-water circulation variability may

D. W. Oppo and J. F. McManus, Department of Geology and Geophysics, Woods Hole Oceanographic Institution, Woods Hole, MA 02543, USA.

J. L. Cullen, Department of Geological Sciences, Salem State College, Salem, MA 01970, USA.